

## Spin-polarized transport in magnetically assembled carbon nanotube spin valves

R. Thamankar, S. Niyogi, B. Y. Yoo, Y. W. Rheem, N. V. Myung, R. C. Haddon, and R. K. Kawakami

Citation: [Applied Physics Letters](#) **89**, 033119 (2006); doi: 10.1063/1.2221910

View online: <http://dx.doi.org/10.1063/1.2221910>

View Table of Contents: <http://scitation.aip.org/content/aip/journal/apl/89/3?ver=pdfcov>

Published by the [AIP Publishing](#)

---

### Articles you may be interested in

[Optimized fabrication and characterization of carbon nanotube spin valves](#)

J. Appl. Phys. **115**, 174309 (2014); 10.1063/1.4874919

[CoFeB spin polarizer layer composition effect on magnetization and magneto-transport properties of Co/Pd-based multilayers in pseudo-spin valve structures](#)

J. Appl. Phys. **113**, 023909 (2013); 10.1063/1.4773336

[Spin-polarized transport in NiFe/perylene-3,4,9,10-tetracarboxylate/Co organic spin valves](#)

J. Appl. Phys. **109**, 07C723 (2011); 10.1063/1.3560907

[Carbon nanotube-based magnetic actuation of origami membranes](#)

J. Vac. Sci. Technol. B **26**, 2509 (2008); 10.1116/1.3002559

[Iron nanoparticle driven spin-valve behavior in aligned carbon nanotube arrays](#)

Appl. Phys. Lett. **93**, 172505 (2008); 10.1063/1.2999374

---



## Spin-polarized transport in magnetically assembled carbon nanotube spin valves

R. Thamankar, S. Niyogi, B. Y. Yoo, Y. W. Rheem, N. V. Myung, R. C. Haddon, and R. K. Kawakami<sup>a)</sup>  
 Center for Nanoscale Science and Engineering, University of California,  
 Riverside, California 92521-0403

(Received 24 February 2006; accepted 25 May 2006; published online 20 July 2006)

Spin polarized transport over 5  $\mu\text{m}$  long carbon nanotubes (CNTs) is observed in magnetically assembled spin valves with electrochemically deposited ferromagnetic (FM) electrodes. An annealing procedure is developed to produce stable devices with highly transmissive FM/CNT contacts. The devices exhibit magnetoresistance (MR) with magnitudes up to 4%, and the sign of MR is consistently negative. The temperature dependence is investigated and MR is observed up to 14 K. Bias dependence is also investigated, with MR persisting up to  $\sim 300$  mV. © 2006 American Institute of Physics. [DOI: 10.1063/1.2221910]

Carbon nanotubes (CNTs) have attracted considerable interest for spin-polarized electronics because their ballistic conductance and low spin-orbit coupling are ideal for coherent spin transport over macroscopic distances.<sup>1-3</sup> Furthermore, the one-dimensional nature of CNT provides a model system to study the behavior of spin in reduced dimensions.<sup>4</sup> Experimental evidence for spin-polarized transport in CNT was first provided by the observation of low-field magnetoresistance (MR) in lateral spin-valve devices [i.e., a CNT bridging two ferromagnetic (FM) electrodes].<sup>5</sup> Recent report of oscillations in the magnitude and sign of MR with gate voltage provides the strongest support that the MR is primarily due to spin-polarized transport.<sup>6</sup>

In this letter, we investigate spin-polarized transport in multiwalled-CNT spin-valve devices produced by a magnetic assembly technique.<sup>7</sup> Postassembly annealing improves the electrical contact between the CNT and the FM electrodes. We observe spin transport over 5  $\mu\text{m}$  with MR magnitudes up to 4% in Co/CNT/Ni and Co/CNT/Co lateral spin valves, and the sign of MR is consistently negative. This is different from what is expected in the Julliere model,<sup>8</sup> and raises interesting questions. In addition, we observe evidence that suspending the CNT may improve spin transport properties, and identify a possible relation between nonlinear current-voltage ( $I$ - $V$ ) characteristics and MR magnitude.

Samples are fabricated by a magnetic assembly technique described in detail elsewhere.<sup>7</sup> Briefly, multiwalled CNTs are grown vertically on  $\text{SiO}_2/\text{Si}$  substrates by chemical vapor deposition (CVD) and Ni caps are deposited onto the free end of the CNT by thermal evaporation. The capped CNTs are released from the substrate and dispersed in a solution of dimethylformamide (DMF) using hexyl amine to exfoliate the van der Waals aggregates. A drop of this CNT solution is placed onto prepatterned Ni, Co, and Au electrodes with geometry shown in Fig. 1(a). The FM electrodes are fabricated by electrodepositing FM thin films on gold electrodes. The magnetic properties of electrodeposited FM films on gold substrates have been investigated by magneto-optic Kerr effect (MOKE). Room temperature magnetic hysteresis loops for electrodeposited Co films typically show sharp magnetization switching but with remanence below

100% [Fig. 1(d), inset]. Ni films also exhibit similar magnetic hysteresis loops. The CNTs are assembled across the electrode gap using an external magnetic field of  $\sim 300$  G. Typically, the FM thicknesses are 200–300 nm, CNT diameters are 50–75 nm, and the number of CNT in a conducting device is between one and four.

The as-assembled devices typically have room temperature resistances above 10 M $\Omega$  [Fig. 1(b)]. In addition to the high contact resistance, we also observe abrupt resistance jumps of several percent a few times each hour. We believe these undesirable electronic properties are related to residual DMF and hexyl amine adsorbed on the CNT. We find that mild anneal at 400 K in a dynamic vacuum of  $10^{-3}$  Torr of inert He gas causes the resistance to steadily decrease over the course of 1 h [Fig. 1(b) shows the final resistance at 400 K], suggesting that a more aggressive annealing procedure could improve the devices.

The optimized annealing procedure is illustrated in the inset of Fig. 1(c). The devices are annealed in Ar/ $\text{H}_2$  (10:1) gas at atmospheric pressure at 675 K for 30 min, followed by a 725 K anneal for 5 min. Notably, atomic force microscopy (AFM) measurements indicate that the CNTs become submerged in the Co and Ni electrodes. We verify that nei-

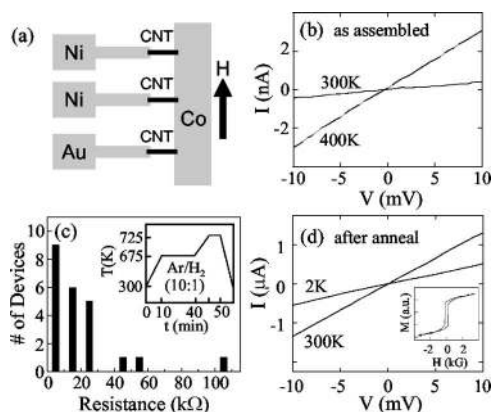


FIG. 1. Device resistance and statistics: (a) Schematic diagram of the FM/CNT/FM devices. (b)  $I$ - $V$  curves for a Co/CNT/Ni device without annealing. (c) Statistical distribution of the two terminal resistance at 300 K. The inset shows the annealing procedure applied to the devices. (d) The  $I$ - $V$  curves for a Co/CNT/Ni device after annealing. Inset: MOKE hysteresis loop for a Co film measured at 300 K.

<sup>a)</sup>Electronic mail: roland.kawakami@ucr.edu

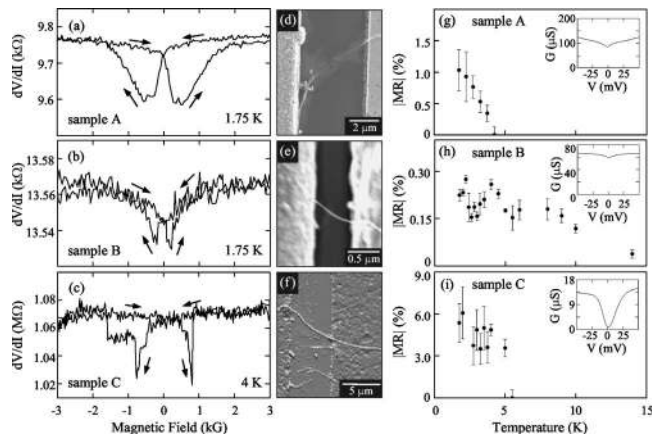


FIG. 2. The transport properties of Co/CNT/Ni devices. (a)–(c) show the two terminal differential resistance measured during the magnetic field scan for samples A, B, and C, respectively. The temperature of measurement is indicated in the inset. The error bar includes uncertainty in the measurements of MR and noise. (d) and (e) show the SEM pictures of samples A and B, while (f) shows the AFM image of the sample C. The gap between the electrodes is also indicated. The temperature dependences of the magnetoresistance are shown in (g)–(i) for the three samples. The insets in (g)–(i) show the two terminal differential resistance measured at 1.75 K.

ther Co nor Ni flows onto the CNT by performing local energy dispersive x-ray spectroscopy in a scanning electron microscope (SEM). After annealing, the room temperature resistance is greatly reduced with most samples below 30 k $\Omega$ , as shown in Fig. 1(c), and the resistance increases by a factor of 2–3 as the device is cooled to 2 K [Fig. 1(d)].<sup>9</sup> Furthermore, the random resistance jumps are largely suppressed. The lowest resistance for a device with a single multiwalled CNT was 6.8 k $\Omega$ ; strong covalent interactions between  $\sigma$ - $\pi$  rehybridized carbon atoms of the CNT and Ni or Co could be responsible for the highly transmissive contacts.<sup>10,11</sup>

Low temperature magnetotransport measurements are performed in a Quantum Design physical property measurement system to control the temperature (1.75–400 K) and magnetic field (up to 14 T). The two terminal differential resistance is measured using standard ac lock-in techniques with an excitation voltage of 100  $\mu$ V. Unless otherwise noted, the differential resistance is measured at zero bias. Magnetic fields are applied in the plane of the device and transverse to the CNT, as shown in Fig. 1(a). Prior to the magnetotransport measurements, the devices are cooled from room temperature to 1.75 K in a magnetic field of 1 T to promote larger FM domains in the presence of surface anti-ferromagnetic oxides.

Figure 2 shows the magnetotransport measurements for three representative Ni/CNT/Co devices whose characteristics are listed in Table I. Figures 2(a)–2(c) show the differential resistance of samples A, B, and C as the magnetic field is swept from  $-3000$  to  $3000$  G and back to  $-3000$  G at a ramp rate of  $\sim 10$  G/s. All three samples exhibit hysteretic curves that are consistent with spin-polarized transport. We operationally define the magnetoresistance as

$$\text{MR} = \frac{[(dV/dI)]_{ap} - [(dV/dI)]_p}{[(dV/dI)]_{ap}},$$

where  $(dV/dI)_{ap}$  and  $(dV/dI)_p$  are the differential resistances of the antiparallel and parallel states, respectively. MR magnitudes up to 4% have been observed in devices with elec-

TABLE I. Physical characteristics of the devices.

Sample	Ni thickness ( $\mu\text{m}$ )	Co thickness ( $\mu\text{m}$ )	Electrode gap ( $\mu\text{m}$ )	No. of CNT
A	0.2	0.2	5	4
B	2.2	2.2	0.5	1
C	0.03	0.03	5	1

trode gap spacing ranging from 0.5 to 5  $\mu\text{m}$ . We are unable to identify any systematic dependence of MR on the gap spacing due to sample-to-sample variations. Devices consisting of one CNT (samples B and C) or multiple CNT (sample A) exhibit MR. The smoother and broader MR curves for sample A (compared to B and C) may be due to the fact that the MR is mostly sensitive to the magnetization of FM domains in direct contact with the CNT, and in sample A the switching characteristics are averaged over many more FM domains due to the multiple CNTs in the device.

Interestingly, all devices in our study show negative MR—the parallel state always exhibits a higher resistance than the antiparallel state. This sample set consists of a total of 17 devices exhibiting MR, including devices undergoing different annealing treatments (i.e., temperature and time) than described in Fig. 1(c). This is in contrast to what one would expect in the simple Julliere model<sup>8</sup> considering the bulk Fermi level spin polarizations of Co and Ni (35% and 23%, respectively, and with the same sign).<sup>12</sup> Thus our observation of negative MR implies additional physical phenomena occurring either at the CNT/FM interfaces or within the CNT itself. We note that earlier work on CNT spin valves has identified positive MR,<sup>5</sup> negative MR,<sup>13</sup> and oscillatory MR as a function of gate voltage.<sup>6</sup> Consequently, we had expected to observe both signs of MR in our sample set. In this context, the consistent observation of negative MR in all our devices is surprising and creates the possibility to systematically investigate its origin. There are several possible explanations for negative MR. One possibility is that oxygen at a Co interface can change the sign of spin polarization.<sup>14</sup> This should result in negative MR for Ni/CNT/Co devices (as observed), but positive MR for Co/CNT/Co devices in Julliere’s model; we, however, observe negative MR in Co/CNT/Co devices. A second possibility is that quantum interferences can change the sign of MR. Sahoo *et al.* observed oscillatory MR as a function of gate voltage and explained their results quantitatively in terms of the quantum interference model.<sup>6</sup> However, in contrast to what we observe, this model allows for both positive and negative MR. While other models have been proposed to explain negative MR,<sup>15,16</sup> in considering their relevance to our study it is important to note the following. DMF, hexyl amine, and ammonia used in the CNT synthesis are all sources of nitrogen,

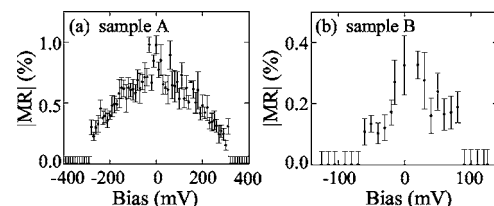


FIG. 3. The bias dependence of magnetoresistance for samples A and B measured at 1.75 K.

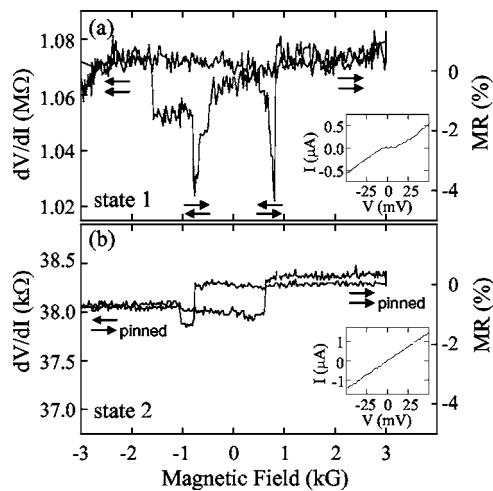


FIG. 4. The evolution of the magnetoresistance in sample C with multiple magnetic field scans. (a) In state 1, the sample showed the highest MR and a clear zero bias anomaly (inset). (b) In state 2, a hysteresis typical of a pinned magnetic layer is observed and the  $I$ - $V$  characteristics are now linear (inset).

which is an  $n$ -type dopant for CNT. While ammonia is known to generate nitrogen defect sites in the CNT lattice, DMF and the amine may incorporate nitrogen into the CNT/FM interface during annealing, so that our devices may be qualitatively different than those studied by other groups.<sup>17</sup> Further studies are needed to explain the origin of the MR behavior in our devices.

The temperature dependence of MR is measured in all the devices and the magnitude of MR is plotted in Figs. 2(g)–2(i). Typically the devices show MR up to 5–6 K. However, in sample B, due to the thickness of the Co and Ni electrodes ( $\sim 2.2 \mu\text{m}$ ), the CNT is found to be freely suspended [Fig. 2(e)] and the MR persists up to 12 K [Fig. 2(h)]. This device structure may have implications for the optimization of CNT spin valves.<sup>18</sup>

The bias dependence of MR for samples A and B is shown in Fig. 3. Both samples exhibit a similar dependence, but the MR persists up to different biases for the two samples. A similar bias dependence was observed previously in Co/CNT/Co devices<sup>19</sup> and multilayer magnetic tunnel junctions.<sup>20</sup> There is no change in the sign of MR in the bias regime studied.

Because sample C has Ni and Co electrodes that are thinner ( $\sim 30 \text{ nm}$ ) than the CNT ( $\sim 50 \text{ nm}$ ), the CNT does not become fully submerged into the electrodes during the annealing process. The thinner FM layers cannot anchor the CNT as effectively as in samples A and B, and we observe that the zero field resistance changes over the course of three days. Figure 4 shows the MR and the  $I$ - $V$  characteristics before and after this change (state 1  $\rightarrow$  state 2). Interestingly, the magnitude of MR ( $\sim 4\%$ ) for state 1 [Figs. 2(c) and 4(a)] is significantly higher than any of the other samples investigated and the  $I$ - $V$  curve exhibits the strongest nonlinearity of all samples [Fig. 4(a)]. In state 2, the MR is reduced to  $\sim 1\%$  and the  $I$ - $V$  curve is nearly linear.<sup>21</sup> Although the shape of the MR curve has changed considerably, it is the expected shape if the CNT is now in contact with a FM domain that is pinned due to exchange bias with an antiferromagnet (e.g., CoO or NiO).<sup>22</sup> Further studies using electrostatic gates and more systematic control of the interfaces are needed to understand the origin of the nonlinear  $I$ - $V$  and its relationship to

the magnitude of MR. Even though the devices with larger gap showed maximum MR, there is no particular dependence of MR on the electrode gap that has been detected in these studies.

For control measurements, we prepare Ni/CNT/Co and Au/CNT/Co devices on the same chip so they can be processed simultaneously. For Ni/CNT/Co, 5 out of 11 conducting devices show MR. For Au/CNT/Co, none of the ten conducting devices shows MR. This suggests that the MR does not arise from single-ended effects as observed recently for (Ga,Mn)As contacts.<sup>23</sup>

In conclusion, we have observed consistently negative MR in magnetically assembled Ni/CNT/Co and Co/CNT/Co spin valves. A postannealing procedure has been developed to improve the device stability and contact resistance between the CNT and FM. Voltage bias and temperature dependence of MR have been investigated. Finally, we find evidence that suspending the CNT may be beneficial for spin-polarized transport and we observe a possible connection between nonlinear  $I$ - $V$  and MR magnitude.

The authors thank Ward Beyermann for technical assistance. This work was supported by DOD/DARPA/DMEA under Grant No. DMEA90-02-2-0216. One of the authors (R.K.K.) acknowledges support from the Research Corporation, ONR, and NSF. Two of the authors (R.T. and S.N.) have contributed equally to this work.

- <sup>1</sup>S. A. Wolf, D. D. Awschalom, R. A. Buhrman, J. M. Daughton, S. von Molnár, M. L. Roukes, A. Y. Chtchelkanova, and D. M. Treger, *Science* **294**, 1488 (2001).
- <sup>2</sup>H. Mehrez, J. Taylor, H. Guo, J. Wang, and C. Roland, *Phys. Rev. Lett.* **84**, 2682 (2000).
- <sup>3</sup>P. Poncharal, C. Berger, Y. Yi, Z. L. Wang, and Walt A. de Heer, *J. Phys. Chem. B* **106**, 12104 (2002).
- <sup>4</sup>M. Bockrath, D. H. Cobden, J. Lu, A. G. Rinzler, R. E. Smalley, L. Balents, and P. L. McEuen, *Nature (London)* **397**, 598 (1999).
- <sup>5</sup>K. Tsukagoshi, B. W. Alphenaar, and H. Ago, *Nature (London)* **401**, 572 (1999).
- <sup>6</sup>S. Sahoo, T. Kontos, J. Furer, C. Hoffmann, M. Gräber, A. Cottet, and C. Schönenberger, *Nat. Phys.* **1**, 99 (2005).
- <sup>7</sup>S. Niyogi, C. Hangarter, R. Thamankar, Y.-F. Chiang, R. Kawakami, N. V. Myung, and R. C. Haddon, *J. Phys. Chem. B* **108**, 19818 (2004).
- <sup>8</sup>M. Juliere, *Phys. Lett.* **54A**, 225 (1975).
- <sup>9</sup>C. Schonenberger, A. Bachtold, C. Strunk, J.-P. Salvetat, and L. Forró, *Appl. Phys. A: Mater. Sci. Process.* **69**, 283 (1999).
- <sup>10</sup>Y. Zhang, N. W. Franklin, R. J. Chen, R. J. Chen, and H. Dai, *Chem. Phys. Lett.* **331**, 35 (2000).
- <sup>11</sup>M. Menon, A. N. Andriotis, and G. E. Froudakis, *Chem. Phys. Lett.* **320**, 425 (2000).
- <sup>12</sup>R. Meserve and P. M. Tedrow, *Phys. Rep.* **238**, 173 (1994).
- <sup>13</sup>B. Zhao, I. Monch, T. Mühl, H. Vinzelberg, and C. M. Schneider, *J. Appl. Phys.* **91**, 7026 (2002).
- <sup>14</sup>K. D. Belaschenko, E. Y. Tsybal, M. V. Schilfgaarde, D. A. Stewart, I. I. Oleynik, and S. S. Jaswal, *Phys. Rev. B* **69**, 174408 (2004).
- <sup>15</sup>A. N. Pasupathy, R. C. Bialczak, J. Martinek, J. E. Grose, L. A. K. Donev, P. L. McEuen, and D. C. Ralph, *Science* **306**, 86 (2004).
- <sup>16</sup>T. S. Kim, *Phys. Rev. B* **72**, 024401 (2005).
- <sup>17</sup>C. P. Ewels and M. Glerup, *J. Nanosci. Nanotechnol.* **5**, 1345 (2005).
- <sup>18</sup>B. J. LeRoy, S. G. Lemay, J. Kong, and C. Dekker, *Nature (London)* **432**, 371 (2004).
- <sup>19</sup>Y. Ishiwata, H. Maki, D. Tsuya, M. Suzuki, and K. Ishibashi, *Phys. Status Solidi C* **2**, 3137 (2005).
- <sup>20</sup>S. O. Valenzuela, D. J. Monsma, C. M. Marcus, V. Narayanmurthi, and M. Tinkham, *Phys. Rev. Lett.* **94**, 196601 (2005).
- <sup>21</sup>C. M. Schneider, B. Zhao, R. Kozhuharova, S. Groudeva-Zotova, T. Mühl, M. Ritschel, I. Mönch, H. Vinzelberg, D. Elefant, A. Graff, A. Leonhardt, and J. Fink, *Diamond Relat. Mater.* **13**, 215 (2004).
- <sup>22</sup>J. Noguees and I. K. Schuller, *J. Magn. Magn. Mater.* **192**, 203 (1999).
- <sup>23</sup>A. Jensen, J. R. Hauptmann, J. Nygard, and P. E. Lindelhof, *Phys. Rev. B* **72**, 035419 (2005).